UDC 531.383:53.088.222 DOI: 10.18698/0236-3933-2020-3-52-65

FINITE-ELEMENT SIMULATION OF THE EIGEN FREQUENCY SPECTRUM OF THE CYLINDRICAL RESONATOR WITH GEOMETRICAL IMPERFECTNESS

M.A. Basarab[1] basarab@bmstu.ru; bmic@mail.ru
B.S. Lunin[2] luninboris@yandex.ru
E.A. Chumankin[3] che54@mail.ru
A.V. Yurin[1] yualex@rambler.ru

[1] **Bauman Moscow State Technical University, Moscow, Russian Federation**
[2] **Lomonosov Moscow State University, Moscow, Russian Federation**
[3] **Joint Stock Company ANPP TEMP-AVIA, Arzamas, Nizhny Novgorod Region, Russian Federation**

Abstract

The solid-state wave gyroscope belongs to the class of the so-called Coriolis vibratory gyroscopes. They are industrially produced, as a rule, in two versions: precise solid-state wave gyroscopes with expensive fused quartz resonators, and devices of low accuracy with metal resonators. The use of metal for the manufacture of a solid-state wave gyroscope resonator for inertial systems of medium and low accuracy can significantly simplify the design of the device and reduce its cost, however, the low-quality factor of the metal resonator and the instability of its dissipative characteristics limit the accuracy characteristics of the solid-state wave gyroscope. The use of high-quality precision fused quartz glass resonators in such solid-state wave gyroscopes is unacceptable because of their high cost. The purpose of the work is to study the characteristics of inexpensive quartz resonators made from industrially produced fused quartz tubes, with the aim of creating a medium-accuracy solid-state wave gyroscope. Using the finite element method, the main types of geometric heterogeneities arising from the production of such resonators and their influence on their spectral characteristics are investigated. The experimental results allow us to draw conclusions about the most significant defects affecting the performance and accuracy of the solid-state wave gyroscopes

Keywords

Solid-state wave gyroscope, finite-element method, FEM

Received 24.03.2020
Accepted 16.04.2020
© Author(s), 2020

Introduction. At present, wave solid-state gyroscopes (SSGs) are widely used. Their action is based on the precession of elastic standing waves in a thin-walled high-quality axisymmetric mechanical resonator under the action of Coriolis forces. The rotation of the wave relative to the resonator is proportional to the external angular displacement; therefore, by analysing the motion of the wave pattern relative to the resonator, the external angular displacement of the SSG is calculated. The resonator is the most critical part of the SSG. It determines the precision of SSG. Resonators of precision SSG are made of quartz glass on precision mechanical equipment [1]. Resonators of low and medium precision devices, for the means of the cost reduction, are made of stainless steel [2]. It is proposed to use industrial quartz tubes for the manufacture of inexpensive SSG resonators in [3–6]. It was demonstrated, that such resonators obtained by simple technology have quite sufficient technical characteristics. The appearance of such a resonator is shown in Fig. 1, it is a segment of a quartz tube, divided by a necking into two parts (an elongated working part and a fixing shank). According to the experiment [3], the necking provides good vibration isolation of the cylindrical working part from the fixed shank, allowing a simple way to obtain resonators with a Q factor of more than 10^6.

Fig. 1. High-Q cylindrical resonator SSG made of industrial quartz tube

At the same time, geometric deviations from the axisymmetric shape of the initial quartz tube will entail a deterioration of other parameters of such resonators, including one of the most important ones — the difference in its eigenfrequencies (frequency splitting).

The frequency splitting (Δf) is the main reason for the random drift of the wave pattern in the SSG; therefore, it is minimized already at the stage of resonator cavity shaping. After manufacturing, the resonator is balanced, reducing the Δf to zero. The larger the Δf value the resonator has after manufacturing, the higher is the complexity of its balancing. Since industrial quartz tubes have a sufficiently large scatter of geometric dimensions, it is advisable to control the geometric dimensions of the tubes used to produce resonators. This will generally reduce the complexity and the cost of balancing.

In our case, the geometry of ideal tubular resonators could be described well by the cylindrical thin-walled shell model, and there are analytical expressions [4] for its own vibration forms. It should be noted that all sorts of geometric defects require the involvement of computer simulations, which is based on the technique of finite elements (FEM). This approach is widely used by various authors both to model the dynamics of the hemispheric quartz SSG (the so-called *wineglass* or *hemispherical resonator gyroscope*, *HRG*) [7–10], and metal cylindrical SSG [11–14]. The FEM method application to the calculation of the dynamics of the "hybrid" quartz resonator, which geometry corresponds to the common metal SSG with a cylindrical resonator being similar to *Innalabs*, is considered in the [15]. The results of dynamic effects modelling of both ideal and imperfect SSG with a resonator in the form of a shell with an arbitrary forming, are represented in [16, 17]. Specialised *ANSYS*, *COMSOL*, and *MATLAB* computer mathematics systems are most commonly used for the course-elemental view.

The dynamics of the SSG type, which is considered in the present work in the form of a fused quartz tube was studied using analytical representations mainly. And defects modelling was done only in the approximation of annular obstacles at the resonator edge [3–5].

The purpose of the work is to determine the described design by finite element simulation of the natural frequency spectrum of a cylindrical resonator in the presence of various shape defects in the original quartz tube (unequal wall thickness, barrel-shaped, etc.) and evaluate the allowable values of these defects.

Problem statement. The solution of the problem is to find the eigenfrequencies and 15 harmonic coordinate functions, which are corresponding to them: six components of the stress tensor σ_{ij}, six components of the strain tensor ε_{ij}, three components of the displacement vector u_i, that satisfy the three equations of motion, six relations between stresses and deformations, six relations between deformations and displacements under homogeneous boundary conditions.

The relation between stress and strain is as follows [18]:

$$\boldsymbol{\sigma} = \mathbf{D}\boldsymbol{\varepsilon}, \tag{1}$$

where $\boldsymbol{\sigma}$ is the stress vector; $\mathbf{D}$ is 6×6 elastic modulus tensor; $\boldsymbol{\varepsilon}$ is elastic strain vector.

Stress and strain tensors consist of *x, y* and *z* normal components and *x-y, y-z* and *z-x* tangent components. Then for an isotropic body (1) could be represented as follows [19]

$$\begin{bmatrix}\sigma_x\\ \sigma_y\\ \sigma_z\\ \sigma_{xy}\\ \sigma_{yz}\\ \sigma_{xz}\end{bmatrix} = \frac{E}{(1+\nu)(1-2\nu)}\begin{bmatrix}1-\nu & \nu & \nu & 0 & 0 & 0\\ \nu & 1-\nu & \nu & 0 & 0 & 0\\ \nu & \nu & 1-\nu & 0 & 0 & 0\\ 0 & 0 & 0 & \frac{1-2\nu}{2} & 0 & 0\\ 0 & 0 & 0 & 0 & \frac{1-2\nu}{2} & 0\\ 0 & 0 & 0 & 0 & 0 & \frac{1-2\nu}{2}\end{bmatrix}\begin{bmatrix}\varepsilon_x\\ \varepsilon_y\\ \varepsilon_z\\ \varepsilon_{xy}\\ \varepsilon_{yz}\\ \varepsilon_{xz}\end{bmatrix}. \quad (2)$$

Here E is the Young's modulus (elastic modulus); ν is Poisson's ratio (transverse compression coefficient).

The equations of motion of an elastic medium are obtained if we equate the force of internal stresses $\nabla\cdot\boldsymbol{\sigma}$ with the product of acceleration $\ddot{\mathbf{u}}$ at the mass per unit volume of the body (i.e., its density) $\rho\ddot{\mathbf{u}}$. Vector form of the equation of motion would be as follows:

$$\rho\ddot{\mathbf{u}} = \nabla\cdot\boldsymbol{\sigma}, \quad (3)$$

where ρ is the volumetric density; $\mathbf{u}$ is the displacement vector.

Equations (1) and (3) form a complete system of partial differential equations for stresses and strains, and the described above boundary conditions should also be added to them.

The equations of motion in displacements are obtained by eliminating the component of the stress tensor $\boldsymbol{\sigma}_{ij}$ from equation (3) using Hooke's law and the relation connecting deformations with displacements:

$$\nabla\cdot\left(\mathbf{c}\nabla\mathbf{u}(\mathbf{r},t)\right) - \rho\ddot{\mathbf{u}} = 0. \quad (4)$$

Here $\mathbf{c}$ is elastic stiffness tensor.

The solution to the equations of motion will be sought in the form

$$\mathbf{u}_i(\mathbf{r},t) = \mathrm{Re}\left(\mathbf{u}_i(\mathbf{r})\,\mathrm{e}^{-j\omega t}\right), \quad (5)$$

where $\mathbf{u}_i(\mathbf{r})$ is only the function of coordinates. Similarly represent the components of the deformation and stress.

We substitute (5) into (4) and taking into account that the external forces and boundary conditions in the case of free oscillations are homogeneous, and the factor $\mathrm{e}^{-j\omega t}$ is reduced, we obtain

$$\nabla\cdot\left(\mathbf{c}\nabla\mathbf{u}_i(\mathbf{r})\right) - k\mathbf{u}_i(\mathbf{r}) = 0, \quad (6)$$

where $k = \rho\omega^2$.

For certain values of k equation (6) has a nonzero solution. The values of $f = \omega/(2\pi)$ correspond to the eigenfrequencies of the elastic vibrations of the resonator, and the functions of $\mathbf{u}_i$ determine the eigenmodes of vibration.

Own modes of vibration have the property of orthogonality. From the condition of orthogonality, it follows, in particular, that the frequencies ω are always real-valued.

Since $\mathbf{u}_i$ are defined only up to an arbitrary constant factor, they can be normalized arbitrarily. Usually it is taken

$$\int_V u_m u_n dV = \delta_{mn}. \tag{7}$$

Here δ_{mn} is the Kronecker delta. Relation (7) expresses the condition of orthonormalization of the natural vibration modes.

For an approximate solution of problem (6), the FEM is used. The calculations were performed in *COMSOL Multiphysics* [20]. This is a powerful interactive environment for three-dimensional modeling of FEM of a large number of scientific and engineering problems based on partial differential equations (PDEs).

During the calculations, the coefficient form of the task of the system of elasticity theory PDEs was used. The system allows carrying out various types of analysis: stationary and transient analysis; linear and nonlinear analysis; analysis of eigenfrequencies.

When solving the *PDE* in *COMSOL Multiphysics*, the software implements finite element analysis based on mesh generation that considers the geometric configuration of bodies, as well as the required calculation error.

Interaction with the program is possible in a standard way — through a graphical user interface (GUI), or by programming with scripts. In the work, a method of interaction through a graphical interface was used.

The resonator structure, chosen for calculations and analysis of eigenfrequencies, is shown in Fig. 2. In modeling, the following geometric dimensions were used: D_1 = 31 mm; $H = (D_1 - D_2) / 2$ = 1.5 mm; L_1 = 22.5 mm; L_2 = 50 mm; L_3 = 15 mm; d = 8 mm.

Results. During the simulation process, the resonator geometry was constructed with the following defects in the location and shape of the end surface of the resonator: ovality; misalignment of the outer and inner cylindrical surfaces; non-perpendicularity of the end of the working part to the axis of the cylindrical surface; non-perpendicularity of the fixed end to the axis of the cylindrical surface.

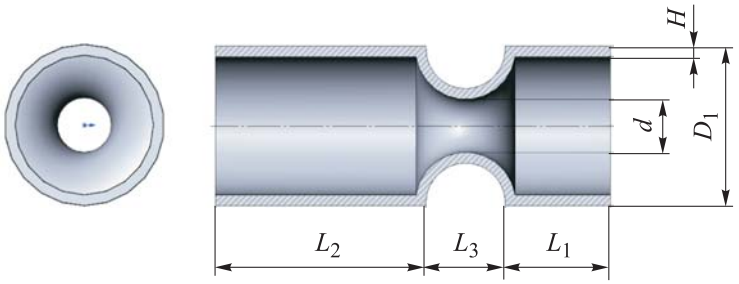

Fig. 2. The resonator structure

In addition, the following deviations of the cross-sectional profile were considered: deviation from rectilinearity of the cylinder axis; conical shape; barrel-shaped; bow effect.

For a resonator with given dimensions and without geometric defects, the spectrum of eigenfrequencies was calculated. During the simulation, a finite element mesh was set mindful of the design features of the resonator (Fig. 3). The calculation results are given below.

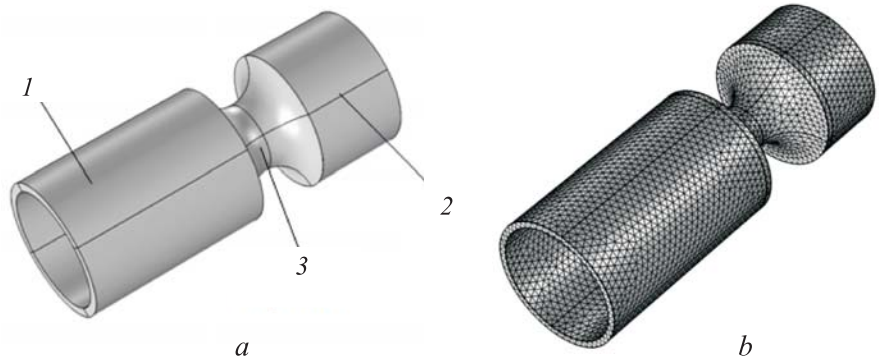

Fig. 3. Three-dimensional model (*a*) and finite element approximation (*b*) of the resonator with no geometry defects:
1 is work area; *2* is shank; *3* is necking

Eigenfrequency spectrum calculation results for the resonator without geometry defects

Frequency, Hz:
- pendulum mode f_1 ..... 989.7
- second flexural mode f_2 ..... 5083.1
- third flexural mode f_3 ..... 13921.3

Frequency splitting, Hz:
- second flexural mode Δf_2 0
- third flexural mode Δf_3 0

The experimental results obtained are correspond with the theoretical estimates, which are made under the assumption of an ideal cylindrical shell [4, 21]:

$$f_n = \sqrt{\frac{\eta\beta^4 + \kappa^2 n^4 (n^2-1)^2}{n^2(n^2+1)}},$$

where n is the number of the vibrational mode ($n = 2$ or $n = 3$);

$$\kappa^2 = \frac{H^2}{3R^2}\eta,\ \eta = \frac{E}{\rho R^2(1-\nu^2)},\ R = \frac{D_1 + D_2}{4},\ \beta \approx 1.875\xi_0^{-1},\ \xi_0 = \frac{L_2}{R}.$$

To find out the degree of influence of the ovality of the cylindrical surface of the resonator (Fig. 4 *a*) on the spectrum of eigenfrequencies and the shape of natural oscillations, finite element simulation was performed for the difference between the major and minor axis of the ellipse Δl, mm: 0.3; 0.6; 0.9; 1.2; 1.6; 1.9; 2.2; 2.5. The values of the main parameters calculated for the considered case are given in Table 1. Based on the data presented, one could come to the conclusion that when one of the semi-axes of the ellipse decreases in the cross section of the tube, the eigenfrequencies increase and the degeneracy of the natural oscillation modes is eliminated.

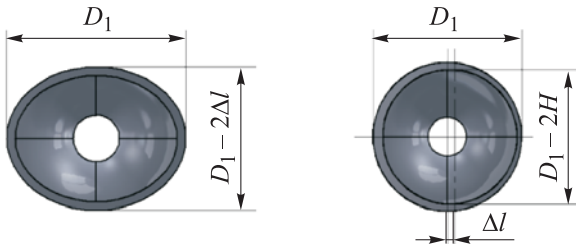

Fig. 4. Cross sections of the resonator with the ovality of the cylindrical surface (*a*) and misalignment of the outer and inner cylindrical surfaces (*b*)

Table 1

The results of calculating the spectrum of eigenfrequencies of the resonator with the ovality of the cylindrical surface at various values of the parameter Δl

Δl, mm	f_1, Hz	f_2, Hz	Δf_2, Hz	f_3, Hz	Δf_3, Hz
0	989.7	5 083.1	0	13 921.3	0
0.3	999.2	5 184.5	1.5	14 205.3	0.1
0.6	1 008.6	5 288.6	5.6	14 497.2	0.3
0.9	1 018.5	5 393.4	13.2	14 790.0	0.9

End of the Table 1

Δl, mm	f_1, Hz	f_2, Hz	Δf_2, Hz	f_3, Hz	Δf_3, Hz
1.2	1 028.3	5 499.5	24.3	15 084.9	1.1
1.6	1 038.6	5 607.2	39.2	15 384.8	1.9
1.9	1 049.1	5 716.4	57.8	15 687.4	2.7
2.2	1 059.4	5 826.7	80.4	15 993.2	5.1
2.5	1 070.1	5 938.6	107.2	16 303.8	9.0

During simulation the misalignment of the outer and inner cylindrical surfaces of the resonator, the displacement parameters Δl, mm, were set (Fig. 4 *b*): 0.125; 0.250; 0.375; 0.500; 0.625; 0.750. The results of calculating the spectrum of eigenfrequencies of the resonator with misalignment of cylindrical surfaces are given in Table 2.

Table 2

The results of calculating the spectrum of eigenfrequencies of the resonator with misalignment of cylindrical surfaces for various values of the parameter Δl

Δl, mm	f_1, Hz	f_2, Hz	Δf_2, Hz	f_3, Hz	Δf_3, Hz
0	989.7	5083.1	0	13921.3	0
0.125	987.3	5078.6	0	13893.0	0.2
0.250	987.1	5065.0	0.3	13805.7	0.1
0.375	983.8	5042.3	1.3	13658.6	1.0
0.500	979.2	5009.1	4.3	13447.1	0.7
0.625	973.5	4965.1	12.1	13167.5	0.4

According to the obtained simulation results, an increase in misalignment of the inner and outer edging circles leads to a decrease in the frequencies observed in the spectrum with maintenance of the oscillating degrees of freedom. The emergent different frequency is associated with the appearance of anisotropy of the transverse stiffness of the resonator. In this regard, there are significant distortions of the modes of transverse oscillations (including the first, second and the third ones). Significant distortions in the shape of such oscillations are already apparent when misalignment is 17 % of the resonator wall thickness.

The calculation of the frequency characteristics of the resonator with the non-perpendicularity of the end surface of the working area (Fig. 5 *a*) to the axis of the cylindrical surface was carried out with the values of the angle of inclination of the end surface $\Delta\varphi$, deg: 0.5; 1.0; 1.5; 2.0; 2.5; 3.0; 3.5; 4.0. The results of calculating the spectrum of eigenfrequencies of a resonator with a

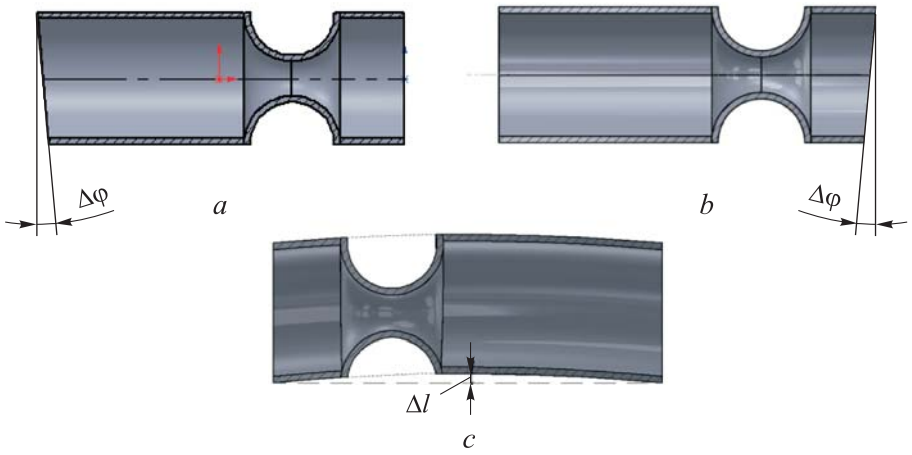

Fig. 5. A resonator with a non-perpendicular end surface of the working part (*a*), with non-perpendicularity of the end surface of the shank (*b*) and with a deviation from rectilinearity of the axis of the cylinder (*c*)

non-perpendicular end surface of the working region to the axis of the cylindrical surface are given in Table 3.

Table 3

The results of calculating the spectrum of eigenfrequencies of the resonator with a non-perpendicular end surface of the working area to the axis of the cylindrical surface for various values of the parameter Δφ

Δφ, deg	f_1, Hz	f_2, Hz	Δf_2, Hz	f_3, Hz	Δf_3, Hz
0	989.7	5083.1	0	13921.3	0
0.5	992.8	5084.2	0.1	13922.2	0.1
1.0	995.9	5085.4	0.1	13923.1	0.2
1.5	999.0	5086.6	0.1	13923.6	0.1
2.0	1002.2	5087.7	0.1	13923.6	0.2
2.5	1005.3	5088.9	0.1	13923.5	0.1
3.0	1008.5	5090.0	0.1	13922.9	0.3
3.5	1011.7	5091.0	0.1	13921.9	0.2
4.0	1014.9	5092.0	0.1	13920.4	0.3

In accordance with the above results, for the cases of the first and second modes of oscillation, with an increase in the parameter Δφ, the values of the eigenfrequencies increase almost linearly, and the resulting frequency difference is tenths of a hertz.

We also investigated in the present work the case with the non-perpendicularity of the end surface of the mounting shank to the cylinder axis (Fig. 5 *b*). It was found out that the occurrence of different frequencies and distortion of the forms of oscillations does not occur.

To establish the effect of a resonator geometry defect in the form of a deviation from the rectilinearity of the cylinder axis, a three-dimensional geometric model of the resonator was constructed with a bend of the axis of the cylindrical surface along a circular arc (Fig. 5 *c*) with a segment height Δl, mm: 0.25; 0.50; 0.75; 1.00; 1.25; 1.50. The results of calculating the spectrum of the eigenfrequencies of the resonator with a deviation from the rectilinearity of the axis of the cylinder are given in Table 4.

Table 4

The results of calculating the spectrum of eigenfrequencies of the resonator with deviation from rectilinearity of the cylinder axis for various values of the parameter Δl

Δl, mm	f_1, Hz	f_2, Hz	Δf_2, Hz	f_3, Hz	Δf_3, Hz
0	989.7	5083.1	0	13921.3	0
0.25	987.5	5085.5	0.7	13934.8	0.2
0.50	987.2	5085.6	0.7	13933.3	0.4
0.75	986.5	5085.7	0.8	13932.5	1.6
1.00	985.7	5085.9	1.1	13931.8	0.9
1.25	983.9	5086.3	1.1	13931.4	0.8
1.50	981.6	5086.9	1.1	13929.1	1.1

As per to the data obtained, resulting the axis bending of the cylindrical surface of the resonator, an increase in the natural frequencies occurs relative to the values calculated for its distortionless shape. In addition, a small frequency difference appears for initially degenerate modes of oscillations.

Considering a cone-shaped axisymmetric defect in the geometry of the resonator, one could distinguish cases of an increase in the radius of the cylindrical surface of the resonator to the end surface and its decrease (expanding and narrowing truncated cone, Fig. 6). The parameter Δl, which determines the taper of the resonator as the difference between the larger and smaller radii on the end surfaces, mm: 0.62; 0.93; 1.24; 1.55; 1.86. The calculated values of the eigenfrequencies of a resonator with a geometry defect in the form of an expanding and tapering truncated cone are given in Table 5.

According to the results of the calculation, a linear dependence of the eigenfrequencies on the change in the Δl parameter is detected, and in case of a

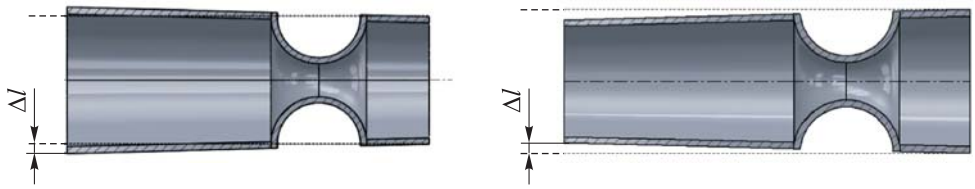

Fig. 6. Conical cavity shape defect:
a, *b* are expanding and tapering truncated cone

defect in the form of an expanding truncated cone, the eigenfrequencies decrease, and in the case of a defect in the form of a tapering one, they increase. The change in eigenfrequencies relative to the values obtained with undistorted resonator geometry is very significant (~10 % at the maximum value of Δ*l*). Thus, significant values of the cone of the resonator lead to noticeable changes in its frequency characteristics without splitting the eigenfrequencies.

Table 5

The results of calculating the spectrum of natural frequencies of the resonator with a conical defect at various values of the parameter Δ*l*

Δ*l*, mm	f_1, Hz	f_2, Hz	f_3, Hz
0	989.7 / 989.7	5083.1 / 5083.1	13921.3 / 13921.3
0.62	949.0 / 1033.3	4925.1 / 5264.6	13499.8 / 14437.4
0.93	930.5 / 1054.8	4847.1 / 5356.4	13282.7 / 14689.9
1.24	913.1 / 1077.1	4771.3 / 5451.8	13071.9 / 14950.9
1.55	895.8 / 1100.1	4698.2 / 5550.3	12868.8 / 15219.7
1.86	878.9 / 1123.8	4627.3 / 5652.1	12670.5 / 15496.0

The numerator shows the values for the geometry defect in the form of an expanding truncated cone, and the denominator shows the values for the tapering one.

Axisymmetric defects such as barrel and bow resonator geometry are considered (Fig. 7). For modeling, the parameter Δ*l*, mm: 0.25; 0.50; 0.75; 1.00; 1.25; 1.50; 2.00. The calculated values of the eigenfrequencies of a resonator with a bow and barrel-shaped geometry defects are shown in Table 6.

The simulation results show an almost linear dependence of the eigenfrequencies on a change in the Δ*l* parameter without the occurrence of a difference in eigenfrequencies. With a barrel-shaped defect in the geometry of the resonator, the decrease in the natural frequencies occurs, and with a bow-shaped defect — the increase occurs. In addition, in the same way as in the

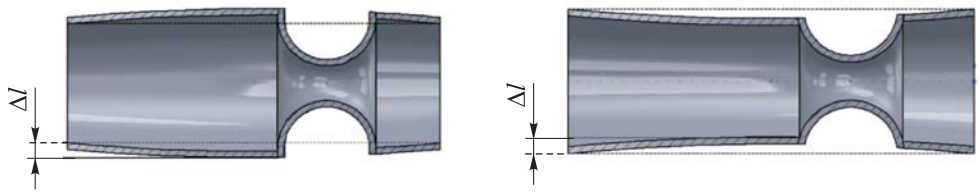

Fig. 7. Resonators with barrel (*a*) and bow (*b*) geometry defects

case of a conical defect in the geometry of the resonator, significant changes in the eigenfrequencies are observed for barrel-shaped and saddle-shaped defects in comparison with their values for undistorted resonator geometry (more than 10 % at the maximum value of Δl).

Table 6

The results of calculating the spectrum of eigenfrequencies of the resonator with geometry defects at various values of the parameter Δl

Δl, mm	f_1, Hz	f_2, Hz	f_3, Hz
0	989.7 / 989.7	5083.1 / 5083.1	13921.3 / 13921.3
0.25	971.1 / 1003.3	5020.8 / 5150.3	13734.4 / 14121.3
0.50	958.0 / 1017.1	4959.7 / 5222.2	13539.8 / 14326.9
0.75	945.0 / 1031.0	4901.8 / 5297.7	13351.0 / 14531.9
1.00	932.5 / 1044.9	4847.0 / 5377.5	13168.9 / 14735.7
1.25	918.6 / 1059.4	4794.6 / 5461.9	12993.4 / 14937.6
1.50	904.7 / 1073.6	4745.1 / 5550.9	12825.5 / 15135.8
2.00	877.7 / 1102.5	4653.5 / 5743.8	12512.5 / 15516.2

The numerator shows values for a resonator with a barrel-shaped geometry defect, and the denominator shows values for a resonator with a bow-shaped geometry defect.

Conclusion. Based on the data obtained, one could come to the conclusion that the greatest influence on the different frequencies of the resonator made of industrial fused quartz tube is exerted by the ovality of its cross section, misalignment of the external and internal cylindrical surfaces and deviation from the straightness of the tube axis. Selecting tubes according to these parameters, one could significantly simplify the procedure for balancing the resonator. The non-perpendicularity of the end surfaces of both the working part and the shank of the resonator affects the frequency split very weakly, and the influence of axisymmetric defects in the geometry of the pipe (conicity, barrel and bow shape) could be neglected.

Translated by K. Zykova

REFERENCES

[1] Remilliex G., Delhaye F. Sagem Coriolis Vibrating Gyros: a vision realized. *DGON ISS*, 2014. DOI: 10.1109/InertialSensors.2014.7049409

[2] Tactical grade gyroscopes. *innalabs.com: website*.
Available at: http://www.innalabs.com/product-category/tactical-grade-gyroscopes (accessed: 21.03.2020).

[3] Lunin B.S., Basarab M.A., Yurin A.V., et al. Fused quartz cylindrical resonators for low-cost vibration gyroscopes. *25th ICINS*, 2018, pp. 291–294.
DOI: https://doi.org/10.23919/ICINS.2018.8405896

[4] Lunin B., Basarab M., Chumankin A., et al. Quartz cylindrical resonators for mid-accuracy Coriolis vibratory gyroscopes. *Proc. IEEE INERTIAL*, 2018, pp. 34–36.
DOI: https://doi.org/10.1109/ISISS.2018.8358120

[5] Basarab M.A., Lunin B.S., Chumankin E.A. Tsilindricheskiy resonator [Cylindric resonator]. Patent RF 187272. Appl. 28.11.2018, publ. 28.02.2019 (in Russ.).

[6] Novozhilov V.V. Teoriya tonkikh obolochek [Theory of thin shells]. St. Petersburg, SPBU Publ., 2010.

[7] Xu Z., Yi G., Qi Z., et al. Structural optimization research on hemispherical resonator gyro based on finite element analysis. *35th Chinese Control Conference (CCC)*, 2016, pp. 5737–5742.

[8] Wei Z., Yi G., Huo Y., et al. The synthesis model of flat-electrode hemispherical resonator gyro. *Sensors*, 2019, vol. 19, iss. 7, art. 1690.
DOI: https://doi.org/10.3390/s19071690

[9] Gao S., Wu J. Theory and finite element analysis of HRG. *2007 Int. Conf. Mechatronics and Automation,* 2007, pp. 2768–2772.
DOI: https://doi.org/10.1109/ICMA.2007.4303997

[10] Pai P., Chowdhury F.K., Pourzand H., et al. Fabrication and testing of hemispherical MESM wineglass resonators. *MEMS*, 2013, pp. 677–680.
DOI: https://doi.org/10.1109/MEMSYS.2013.6474333

[11] Lunin B.S., Basarab M.A., Matveev V.A., et al. Resonator materials for Coriolis vibratory gyroscopes. *Proc. 22th Saint Petersburg Int. Conf. on Integrated Navigation Systems*. St. Petersburg, 2015, Concern CSRI "Elektropribor", pp. 379–382 (in Russ.).

[12] Basarab M.A., Lunin B.S., Matveev V.A., et al. Miniature gyroscope based on elastic waves in solids for small spacecraft. *Herald of the Bauman Moscow State Technical University, Series Instrument Engineering*, 2014, no. 4 (97), pp. 80–96 (in Russ.).

[13] Matveev V.A., Basarab M.A., Lunin B.S., et al. Development of the theory of cylindrical vibratory gyroscopes with metallic resonators. *Vestnik RFFI* [Russian Foundation for Basic Research Journal], 2015, no. 3 (87), pp. 84–96 (in Russ.).

[14] Naraykin O.S., Sorokin F.D., Kozubnyak S.A., et al. Numerical simulation of elastic wave precession in the cylindrical resonator of a hemispherical resonator gyroscope featuring a non-homogeneous density distribution. *Herald of the Bauman Moscow State Technical University, Series Mechanical Engineering*, 2017, no. 5 (116), pp. 41–51 (in Russ.). DOI: https://doi.org/10.18698/0236-3941-2017-5-41-51

[15] Pan Y., Wang D., Wang Y., et al. Monolithic cylindrical fused silica resonators with high Q factors. *Sensors*, 2016, vol. 16, iss. 8, art. 1185.
DOI: https://doi.org/10.3390/s16081185

[16] Vakhlyarskiy D.S., Guskov A.M., Basarab M.A., et al. Using a combination of FEM and perturbation method in frequency split calculation of a nearly axisymmetric shell with middle surface shape defect. *Nauka i obrazovanie: nauchnoe izdanie MGTU im. N.E. Baumana* [Science and Education: Scientific Publication], 2016, no. 5 (in Russ.). DOI: http://dx.doi.org/10.7463/0516.0839190

[17] Vakhlyarskiy D.S., Guskov A.M., Basarab M.A., et al. Numerical study of differently shaped HRG resonators with various defects. *Nauka i obrazovanie: nauchnoe izdanie MGTU im. N.E. Baumana* [Science and Education: Scientific Publication], 2016, no. 10 (in Russ.). DOI: http://dx.doi.org/10.7463/1016.0848188

[18] Lunin B.S., Yurin A.V., Basarab M.A., et al. Thermoelastic losses in structural materials of wave solid-state gyroscope resonators. *Herald of the Bauman Moscow State Technical University, Series Instrument Engineering*, 2015, no. 2 (101), pp. 28–39 (in Russ.). DOI: https://doi.org/10.18698/0236-3933-2015-2-28-39

[19] Mitchell A.R., Wait R. The finite element method in partial differential equations. Wiley, 1977.

[20] COMSOL Multiphysics® Modeling Software. Available at: http://www.comsol.com (accessed: 21.03.2020).

[21] Chumankin E.A., Lunin B.S., Basarab M.A. Features of balancing metal resonators of solid-state wave gyroscopes. *Dinamika slozhnykh sistem — XXI vek* [Dynamics of Complex Systems — XXI century], 2018, no. 4, pp. 85–95 (in Russ.).

Basarab M.A. — Dr. Sc. (Phys.-Math.), Assoc. Professor, Department of Information Security, Bauman Moscow State Technical University (2-ya Baumanskaya ul. 5, str. 1, Moscow, 105005 Russian Federation).

Lunin B.S. — Dr. Sc. (Eng.), Leading Researcher, Chemistry Faculty, Lomonosov Moscow State University (Leninskie gory 1, str. 3, GSP-1, Moscow, 119991 Russian Federation).

Chumankin E.A. — Cand. Sc. (Eng.), Deputy Chief of Division, Joint Stock Company ANPP TEMP-AVIA (Kirova ul. 26, Arzamas, Nizhny Novgorod Region, 607220 Russian Federation).

Yurin A.V. — Scientific Researcher, Scientific and Educational Complex Informatics and Control Systems, Bauman Moscow State Technical University (2-ya Baumanskaya ul. 5, str. 1, Moscow, 105005 Russian Federation).

Please cite this article as:

Basarab M.A., Lunin B.S., Chumankin E.A., et. al. Finite-element simulation of the eigen frequency spectrum of the cylindrical resonator with geometrical imperfectness. *Herald of the Bauman Moscow State Technical University, Series Instrument Engineering*, 2020, no. 3 (132), pp. 52–65. DOI: https://doi.org/10.18698/0236-3933-2020-3-52-65